Politecnico di Torino

Dipartimento di Elettronica e Telecomunicazioni
Master Degree in Biomedical Engineering
A.a 2023/2024
Marzo 2024

Automatic Spike and Wave identification in the EEG of epileptic patients for the prediction of epileptic seizures

Supervisor:

Prof./Dr. Luca Mesin

Submitted by:

Gianlorenzo Di Iasio

Abstract

To analyse epileptic seizures, EEG signals are fundamental for neurologists to diagnose pathological events and evaluate medical treatments. Doing so is not very time-efficient, so an automatic method is required for faster analysis. The basis for this method is the pathological event of the spike and wave, which is indicative for epilepsy. The objective of this study is the ideation of a spike and wave detector based on a set of prototypes spike and waves and match filters to support the diagnosis of epilepsy and predict the incoming attack with the detection of spike and waves in EEG signals. The first section provides a brief anatomical, physiological and biological introduction to the central nervous system, essential to understand the fundaments of the epileptic seizures. A brief description of seizures and their classifications is also provided, along with their pathological waveforms shown in EEG recordings. The second section is dedicated to the state of the art, exploring the many algorithms dedicated to the identification of spike and waves in EEG recordings. The third section describes the dataset used in this study and each individual step of the algorithm developed for this research. The results achieved are explained in the fourth section.

Contents

List of Figures

List of Tables

Chapter 1

Introduction

In biology, the nervous system is the one of the most complex part of an animal, its main feature is to generate and coordinate actions and sensory information with signals. To understand these signals, one of the main methods is electroencephalography, a non-invasive technique which records the spontaneous electrical activity of the brain.

1.1   The Central Nervous System

The central nervous system (CNS) is a crucial component of the overall nervous system in vertebrates, including humans. It serves as the primary control and processing center for information within the body. The CNS is composed of two main structures: the brain and the spinal cord[1].

1. **Brain**

   - The **brain** is the most complex and vital organ in the CNS.
   - It is located within the cranial cavity of the skull and is protected by layers of membranes (meninges) and cerebrospinal fluid.
   - The brain is divided into several major parts, including the **cerebrum**, **cerebellum**, and **brainstem**.

2. **Spinal Cord**

   - The **spinal cord** is a long, tubular structure that extends from the base of the brain (brainstem) down the vertebral column.
   - It is encased in the vertebral column's bony structures, which provide protection.
   - The spinal cord serves as a pathway for nerve impulses traveling to and from the brain and peripheral nerves.
   - It is responsible for reflex actions, quick, automatic responses to stimuli that don't require conscious thought.

3. **Function**

   - The central nervous system is the main processing unit for sensory information, integrating signals from the body and external environment.
   - It is involved in generating motor responses and coordinating voluntary and involuntary actions.
   - The CNS is crucial for higher cognitive functions, including learning, memory, reasoning and emotion.
   - It plays a vital role in maintaining homeostasis, regulating the body's internal environment.

4. **Communication**

   - Neurons, the basic units of the nervous system, transmit electrical impulses and chemical signals within the CNS.
   - Synapses, specialized junctions between neurons, facilitate communication by utilising neurotransmitters.

5. **Integration**

   - The CNS integrates information from various sensory organs and coordinates responses to stimuli, ensuring appropriate reactions to changes in the environment or within the body.
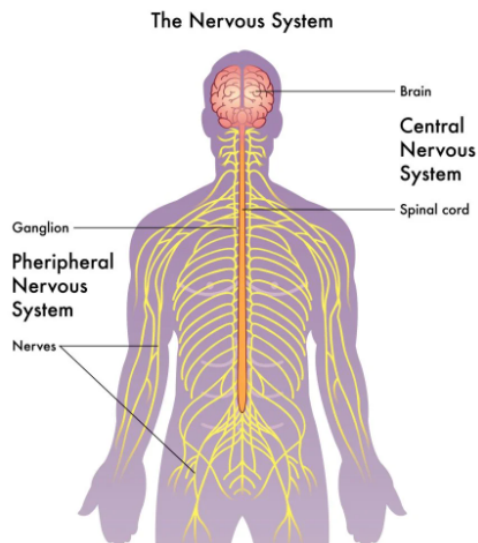
Figure 1.1.1: The nervous system

For this study, it's better to focalize our attention on the brain, since it's the only organ in the nervous system where epilepsies generate.

1.1.1 Brain anatomy
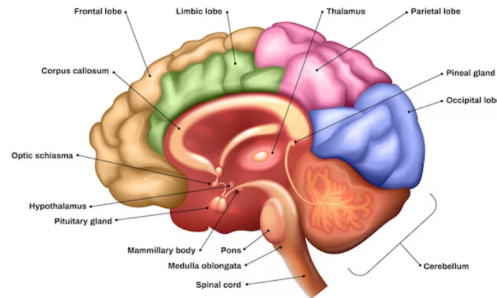
Figure 1.1.2: The brain

The brain is a highly complex and intricate organ that serves as the control center for the nervous system in most animals, including humans. It is a vital part of the central nervous system and plays a crucial role in regulating and coordinating various physiological and cognitive functions[2]. Here are the key aspects of the human brain:

1. **Structure**:

   - **Cerebrum**: The largest part of the brain, responsible for higher cognitive functions such as thinking, memory, reasoning, and perception. It is divided into two hemispheres (left and right) and is further divided into lobes, including the frontal, parietal, temporal, and occipital lobes.
   - **Cerebellum**: Located at the back of the brain, the cerebellum is involved in coordination, balance, and motor control.
   - **Brainstem**: Connects the brain to the spinal cord and is responsible for basic life functions such as breathing, heart rate, and digestion. It includes the medulla oblongata, pons, and midbrain.

2. **Neurons and Synapses**:

   - The brain is composed of billions of neurons, the basic building blocks of the nervous system. Neurons communicate with each other through synapses, which are specialized junctions where neurotransmitters transmit signals from one neuron to another.

3. **Hemispheres and Lobes**:

   - The left hemisphere is often associated with logical and analytical functions, while the right hemisphere is linked to creativity and spatial abilities. Each hemisphere controls the opposite side of the body.
   - Different lobes of the brain have specialized functions. For example, the frontal lobe is associated with decision-making and motor functions, the parietal lobe with sensory perception, the temporal lobe with auditory processing, and the occipital lobe with vision.

4. **Functions**:

   - **Cognition**: The brain is responsible for cognitive functions such as learning, memory, attention, and problem-solving.

   - **Emotion**: The limbic system, a set of structures within the brain, plays a key role in emotions and emotional responses.

   - **Motor Control**: The brain, particularly the motor cortex, is involved in planning and executing voluntary movements.

   - **Sensory Processing**: Different regions of the brain process sensory information, allowing us to perceive and interpret the world around us.

5. **Protection**:

   - The brain is well-protected by the skull, meninges (protective membranes), and cerebrospinal fluid, which cushions and nourishes the brain[3].

6. **Plasticity**:

   - The brain exhibits a degree of plasticity, allowing it to reorganize and adapt in response to experiences, learning and injuries. Understanding the complexity and functionality of the brain is an ongoing area of research, and scientists continue to explore its mysteries to gain insights into neurological disorders, cognitive processes and human behavior. To reach this objective, it's important to analyze the basic units of the CNS, the neurons[4].
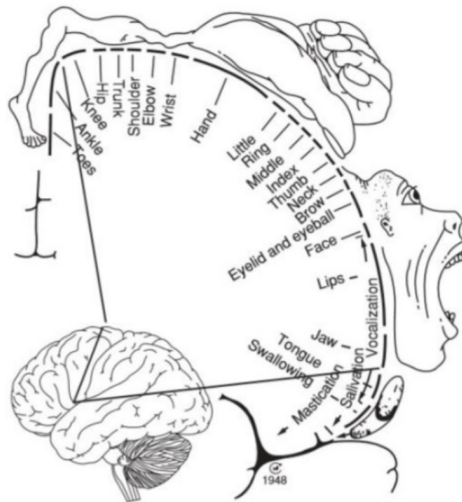
Figure 1.1.3: The motor homunculus derived by Wilder Penfield illustrating the effects of electrical stimulation of the cortex of human neurosurgical patients

1.1.2   The Neurons

A **neuron** is a specialized cell that is fundamental to the structure and function of the nervous system. Neurons are the primary building blocks of the nervous system and are responsible for transmitting information in the form of electrical impulses[5].

1. **Key Components**:

   - **Cell Body (Soma):** Contains the nucleus and other organelles essential for the cell's metabolic functions.
   - **Dendrites:** Branching extensions that receive signals from other neurons or sensory receptors.
   - **Axon:** Long, slender projection that carries the neuron's output away from the cell body.
   - **Axon Terminals (Terminal Buttons):** Small structures at the end of the axon containing vesicles filled with neurotransmitters.
   - **Synapse:** Small gap between the axon terminals of one neuron and the dendrites or cell body of another neuron.

2. **Function**: The transmission of information between neurons is primarily electrical in nature. When a neuron is activated, an electrical impulse, known as an action potential, travels down its axon. At the synapse, neurotransmitters are released, facilitating the transmission of signals to other neurons or target cells.
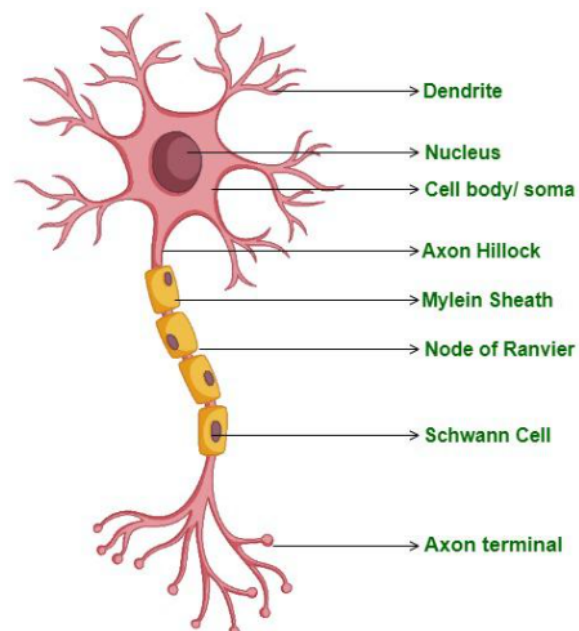
Figure 1.1.4: Diagram of a Neuron

1.1.3 Physiology of the Nervous System: the Action Potential

An **action potential** is a crucial electrochemical event that occurs in neurons, facilitating the rapid transmission of signals along the length of the cell. This process involves a series of stages, each tightly regulated by the movement of ions across the neuron's membrane[6].

Stages of an Action Potential

1. **Resting State:**

   - The neuron is at rest, maintaining a stable resting membrane potential.
   - The membrane is selectively permeable, with higher concentrations of sodium ions ($Na+$) outside the cell and potassium ions ($K+$) inside.
   - Voltage-gated sodium and potassium channels are closed.

2. **Depolarization:**

   - A stimulus, often from a neurotransmitter binding to receptors, triggers the opening of specific ion channels.
   - Voltage-gated sodium channels open, allowing a rapid influx of $Na+$ ions.
   - This influx causes a change in membrane potential, making the interior of the cell more positive (depolarization).

3. **Threshold:**

   - If the depolarization reaches a critical threshold (typically around -55 mV), voltage-gated sodium channels open more widely, initiating the action potential.

4. **Rising Phase:**

   - Voltage-gated sodium channels open extensively, resulting in a rapid increase in membrane potential (rising phase).
   - The interior of the cell becomes highly positive.

5. **Falling Phase:**

   - After reaching its peak, voltage-gated sodium channels begin to inactivate, and voltage-gated potassium channels open.
   - Potassium ions ($K+$) move out of the cell, repolarizing the membrane and restoring a negative charge.

6. **Undershoot:**

   - Brief hyperpolarization occurs as potassium channels remain open briefly, causing the membrane potential to dip below the resting state.
   - During this refractory period, the neuron is less responsive to additional stimuli.

The action potential ensures the rapid and unidirectional transmission of signals along the length of a neuron, allowing for efficient communication within the nervous system.
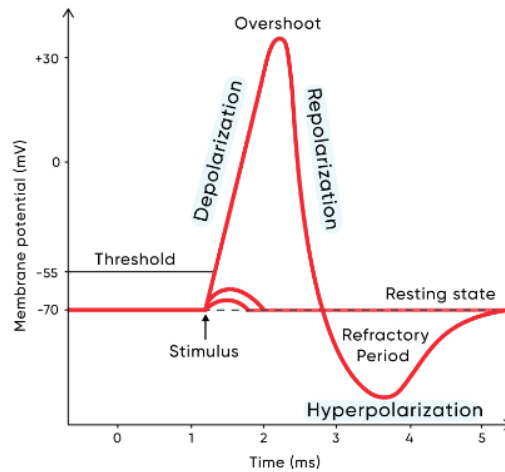
Figure 1.1.5: Stages of an Action Potential

1.2 Epilepsy

Epilepsy Overview

Epilepsy is a neurological disorder characterized by recurrent, unprovoked seizures. Seizures result from abnormal electrical activity in the brain, leading to temporary disruptions in normal brain function. Epilepsy can affect individuals of any age and its severity and manifestations vary widely[7].

1.2.1 Causes

Epilepsy can be idiopathic (unknown cause) or result from various factors, including genetic predisposition, brain injury, infections, developmental disorders or brain abnormalities.

1.2.2 Types of Seizures

Epileptic seizures are categorized into two main types[8]:

1. **Focal (Partial) Seizures**:

   - Originate in a specific area of the brain.
   - Subtypes include simple partial seizures (affecting a specific part of the brain without loss of consciousness) and complex partial seizures (involving altered consciousness).

2. **Generalized Seizures**:

   - Involve widespread areas of the brain.
   - Types include absence seizures (brief loss of consciousness), tonic-clonic seizures (previously known as grand mal seizures), atonic seizures (loss of muscle tone) and myoclonic seizures (brief muscle jerks).

1.2.3 Manifestations of Epilepsy

1. **Aura**:

   - Some individuals experience a warning sign or aura before a seizure, which can manifest as a specific sensation, emotion or altered perception.

2. **Focal Onset Aware Seizures**:

   - Previously known as simple partial seizures.
   - Consciousness remains intact.
   - Symptoms depend on the part of the brain affected and can include altered senses, twitching, or repetitive movements.

3. **Focal Onset Impaired Awareness Seizures**:

   - Previously known as complex partial seizures.
   - Altered consciousness or awareness.
   - May involve automatic, repetitive behaviors.

4. **Absence Seizures**:

   - Brief episodes of staring or "spacing out."
   - Common in children.
   - No memory of the episode afterward.

5. **Tonic-Clonic Seizures**:

   - Involves both tonic (stiffening) and clonic (jerking) phases.
   - Loss of consciousness.
   - Often followed by confusion or fatigue.

6. **Atonic Seizures**:

   - Sudden loss of muscle tone.
   - Can result in falls.

7. **Myoclonic Seizures**:

   - Brief, involuntary muscle jerks.
   - Can affect specific muscles or the entire body.

8. **Status Epilepticus**:

   - Prolonged or repeated seizures without full recovery between episodes.
   - Requires emergency medical attention.

1.2.4 Diagnosis and Treatment

Diagnosis involves medical history, neurological exams, imaging studies, and electroencephalogram (EEG) tests. Treatment often includes antiepileptic medications, lifestyle modifications, and, in some cases, surgery[9].

1.2.5 Impact on Daily Life

Epilepsy can have a significant impact on daily activities, driving restrictions, employment, and social interactions. However, with proper management, many individuals with epilepsy lead full and productive lives.

1.3 Electroencephalography

An EEG test [10] works by measuring the electrical activity generated by the neurons in the brain. Neurons communicate with each other mainly through electrical impulses, creating a small amount of electrical voltage. When many neurons are activated simultaneously, the cumulative electrical activity can be detected on the scalp using electrodes.

1.3.1 Key Steps in EEG Measurement

1. **Electrode Placement** :

   - Small metal electrodes are strategically placed on the scalp. The locations follow an international system (e.g., 10-20 system) to ensure consistency across recordings.
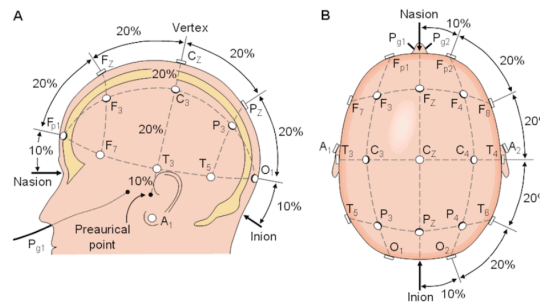
Figure 1.3.1: 10-20 system

2. **Electrical signals detection**:

   - The electrodes detect the electrical signals produced by the synchronized activity of groups of neurons.

3. **Amplification**:

   - The weak electrical signals detected by the electrodes are amplified to create a more readable and analyzable signal.

4. **Recording**:

   - The amplified signals are recorded over time, creating a visual representation known as an EEG waveform or tracing.

5. **Signal analysis**:

   - The recorded EEG is then analyzed for various patterns, frequencies, and abnormalities.

1.3.2 Frequency Bands Analyzed in EEG

The EEG signal is composed of different frequency bands, each associated with specific brain states and activities:

1. **Delta** (0.5-4 Hz):

   - Predominant during deep sleep.
   - Abnormalities may indicate brain damage.

2. **Theta** (4-8 Hz):

   - Present during drowsiness and the early stages of sleep.
   - Abnormalities may be associated with certain brain disorders.

3. **Alpha** (8-13 Hz):

   - Predominant during wakeful relaxation with eyes closed.
   - Suppressed with eye opening.
   - Abnormalities may indicate certain brain disorders.

4. **Beta** (13-30 Hz):

   - Present during wakefulness and periods of increased mental activity.
   - Higher frequency beta waves are associated with alertness and concentration.

5. **Gamma** (30+ Hz):

   - Associated with complex cognitive processes, including perception and consciousness.

1.3.3 Applications of EEG

1. **Epilepsy Diagnosis and Monitoring**:

   - Identifying abnormal patterns associated with seizures.

2. **Sleep Disorders**:

   - Assessing sleep stages and diagnosing sleep disorders.
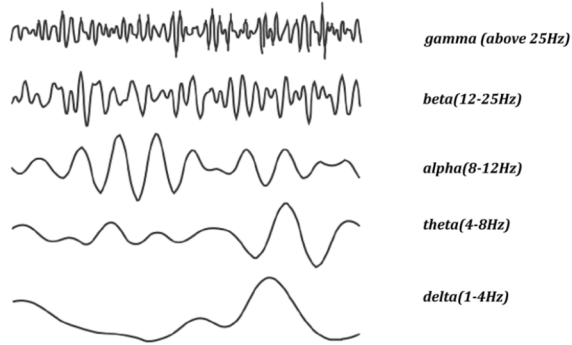
Figure 1.3.2: Frequency bands of EEG signal

3. **Brain Injury and Disorders**:

   - Detecting abnormalities associated with traumatic brain injury, stroke, tumors, and various neurological disorders.

4. **Research**:

   - Studying brain function, cognitive processes, and neurological mechanisms.

5. **Neurofeedback**:

   - Used in biofeedback interventions to train individuals to control certain brainwave patterns.

EEG is a versatile tool employed in neurology, clinical medicine, sleep medicine, and research to gain insights into brain function and diagnose a range of neurological conditions. The patterns and frequencies observed in the EEG provide valuable information about the brain's electrical activity and can aid in understanding various neurological phenomena.

1.4 EEG Waveform Abnormalities: Spike-and-Wave Patterns

Electroencephalograms are essential for detecting abnormal electrical patterns in the brain. Certain waveform abnormalities, such as spike-and-wave patterns [11], are particularly significant and often associated with specific neurological conditions. Below is a detailed description of spike-and-wave patterns and their clinical implications.

1.4.1 Spike-and-Wave Patterns

1. **Description:**

   - A spike-and-wave pattern on an EEG consists of a sharp, often pointed, deflection followed by a slower wave.

- Typically, these patterns are brief, lasting only a fraction of a second.

2. **Clinical Significance:**

   - Strongly associated with epilepsy, particularly generalized epilepsies.
   - Commonly observed in conditions such as absence seizures (formerly known as petit mal seizures).

3. **Absence Seizures:**

   - Hallmark of absence seizures, characterized by a brief loss of consciousness and awareness.

4. **Duration and Frequency:**

   - The duration and frequency of spike-and-wave patterns can vary, and their presence may be intermittent.

5. **Location on EEG:**

   - The specific location of spike-and-wave patterns on the EEG provides additional information about the seizure focus.

6. **Activation Procedures:**

   - Spike-and-wave patterns may be more easily provoked or intensified by specific activation procedures, such as hyperventilation or photic stimulation.

1.4.2   Other EEG Abnormalities

1. **Sharp Waves:**

   - Similar to spikes but with a slower onset.
   - May indicate abnormal brain activity and are associated with various conditions, including focal epilepsies.

2. **Poly-Spikes:**

   - Multiple, often high-frequency spikes occurring together.
   - Seen in certain epilepsy syndromes, such as Lennox-Gastaut syndrome.

3. **Slow Waves:**

   - Abnormal, often rhythmic slow waves in the EEG.
   - Can indicate underlying brain dysfunction, structural abnormalities, or encephalopathy.

4. **Sharp-and-Slow Waves:**

   - A combination of sharp waves followed by slower waves.
   - May be seen in specific seizure types or epilepsy syndromes.

5. **Frontal or Temporal Spikes:**

   - The location of spikes on the EEG can provide information about the origin and potential focus of abnormal brain activity.

1.4.3 Clinical Management

- Identification of spike-and-wave patterns in an EEG is crucial for diagnosing and managing epilepsy.

- Treatment may involve antiepileptic medications, lifestyle modifications, and, in some cases, surgical intervention.
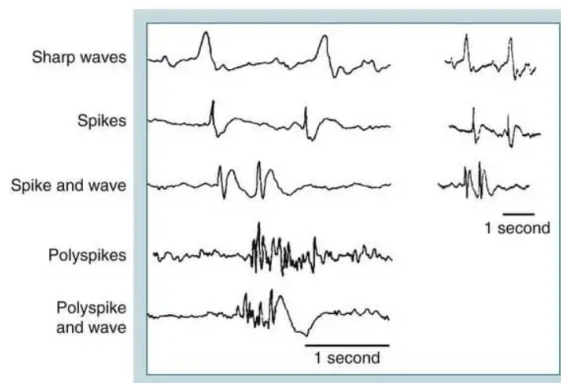
Figure 1.4.1: Different types of spikes seen on the EEG

Chapter 2

State of the art

Since the 1970s, scientists have been trying to develop a reliable, efficient and automatic epileptiform spike and wave detection algorithm. Alas, even with better and faster tools, a method for unsupervised detection of clinically reliable spike and waves has yet to be developed. Various automatic spike and wave detection have been proposed, the algorithms are usually categorized in the following classes:

- Template matching
- Mimetic analysis
- Power spectral analysis
- Wavelet analysis
- Artificial networks
- Fuzzy clustering
- Chaos theory
- Nonlinear Dynamic System
- Matched filtering, which inspired this study

2.1 Template Matching

One example of this algorithm is provided by the study "Improved Spike Detection Algorithm Based on Multi-Template Matching And Feature Extraction"[12]. In this research, putative spike detection of average reference (AV) channels is done by following these steps.

2.1.1 Universal Template Matching

Spikes are detected based on spike morphological similarity between EEG signal frames and template waveforms. This kind of approach focuses on linear time complexity of the data size of the EEG signals. A EEG signal frame is labeled as a possible putative spike when a certain similarity threshold is reached.

2.1.2 Epoch division, feature extraction and spikes eliminated by the threshold

Spike and waves can also be classified as benign (as in non associated with epileptic seizures)[13], so a feature extraction and a threshold method are used to filter the benign variants. An epoch of 150 ms is established to divide the wave sequence of the putative spike. Two features of the putative spikes, slope of left half wave of spike (LH) and slope of right half wave of spike (RH) are extracted to distinguish a spike from the background. Then the spikes are filtered by the feature threshold, to reduce the computational load of spike and wave classification.

2.1.3 Clustering and Candidate Detection

To classify the remaining putative spikes, a k-means algorithm is used to calculate the various centroids of the several clusters. These centroids are then used as new template waveforms to perform a new template matching to find new possible candidate spikes with new thresholds, filtering the false positives spike and waves.
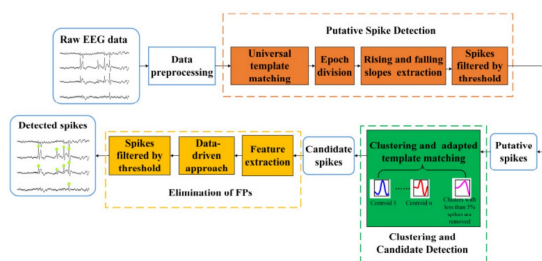
Figure 2.1.1: Detailed workflow of the example of template matching algorithm

2.1.4 Conclusions

While this method is very efficient and doesn't require a heavy computational load, not all detected spikes are true spikes and, to optimize the precision of the algorithm, parameter settings for individual medical doctors are required.

2.2 Mimetic Analysis

In the research "EEG transient event detection and classification using association rules" [14] this kind of algorithm is perfectly explained.
Mimetic methods are based on the concept that automatic EEG analysis should be equal to the visual analysis made by expert in the daily practices, so they should be able to distinguish spike and wave in background activity and associate possible spike and waves with template based techniques. For this purpose, the association rule mining technique has already been introduced [15]. This methodology mines reproducible activation patterns in epileptic EEG signals, as explained in the following procedures.

2.2.1 First stage: Signal processing

The background activity is filtered and transient events are detected in EEG signals. The background activity was filtered with the use of a variable threshold calculated on the values of the EEG signal in a window of constant length.

2.2.2 Second stage: Clustering of transient events and feature extraction

The inputs of the cluster are the transient events and the outputs of said cluster are the prototype transient events. This procedure emulates the kind of logical reasoning that the neurologists follow during the examination of EEG signals. Also, with clustering, we discover the many types of transient events in an EEG recording. To reproduce the outputs, the minimization of the regularized cost function[16] is applied. Sixteen features are also extracted, like duration, area, average slop, sharpness, standard deviation and dominant frequency, just to name a few.

2.2.3 Third stage: Discretization and feature selection

At this point, the continuous valued features are discretized for the use of the selected classification association rule mining technique. The discretization is made possible with entropy minimization and minimum description length principle[17]. For dimensionality reduction, only a selected number of discretized features are chosen, a filter approach is chosen for this objective.

2.2.4 Fourth stage: Classification using association rules

For this final procedure, several algorithms are tested. In short, classification using association rules employs those rules, called class association rules, and, after their generation, they are used to generate a classification model.
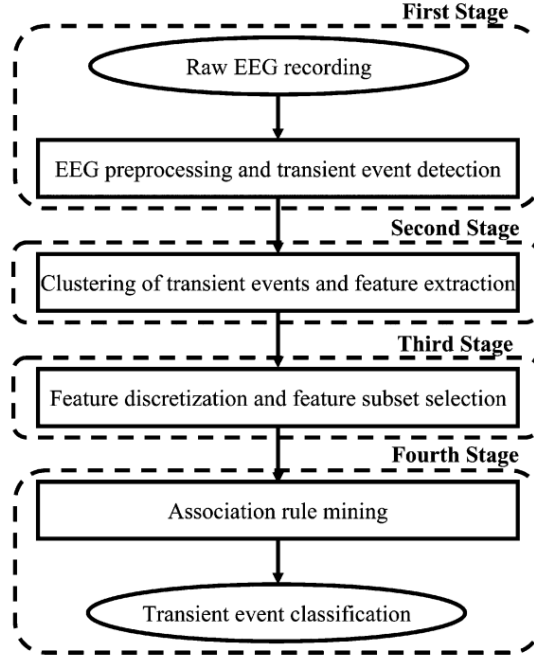
Figure 2.2.1: Detailed workflow of the example of mimetic analysis algorithm

2.2.5 Conclusions

While this method has a high enough accuracy, a clear limitation is the employment of association rules for the classification. While their use allows to find valid, causal relationships in the clinical data, these rules can also find spurious and particular relationships among the data in the specific dataset. Another limitation stems from the number of features extracted.

2.3 Power Spectral Analysis

There are many works involving this kind of approach, "The Use of Time-Frequency Distributions of Epileptic Seizure Detection in EEG Recordings"[18] is one of them. In this study, time-frequency analysis is performed since it is particularly effective for representing the aspects of nonstationary signals such as spike and wave.

2.3.1 Time-frequency Analysis

Short-time-Fourier-Transform (STFT) and various Time-Frequency-Distributions (TFD) are used for the time-frequency analysis of the EEG recordings. For the purpose of this study, the Cohen's class of distribution[19] is used. Using time-frequency analysis, the power spectral density (PSD) is calculated.

2.3.2 Feature Extraction

The PSD computed in the previous procedure is used to extract several features: frequencies are divided into subbands, so that the features can be calculated from the PSD found in these subbands. In short, each feature represents the fractional energy of the signal in a specific frequency band and time window, so the feature set is the distribution off the signal's energy in the time-frequency plane. This procedure is done to extract significant information related to the non-stationary properties of the EEG signal.
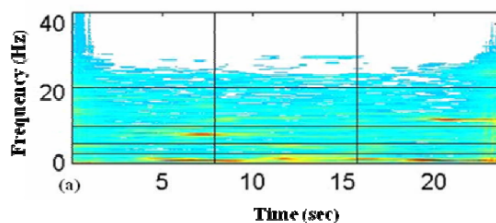
Figure 2.3.1: PSD with grid for feature extraction

2.3.3 Classification

The calculated features are used as inputs for a feed-forward artificial neural network (ANN). The ANN is composed of N inputs, one hidden layer of $5 * N$ neurons, with sigmoid units with hyperbolic tangent as activation function and linear outputs as the units in the hidden layer. Each network is trained with a backpropagation algorithm.

2.3.4 Conclusions

The accuracy of this algorithm is more than satisfactory, but the method mainly works with predetermined EEG segments, with a certain length. Applying this method into long time EEG recordings and classify them may achieve different results. Also, it performs poorly in a low SNR environment.

2.4 Wavelet Analysis

The "A Novel Wavelet Based Algorithm for Spike and Wave Detection in Absence Epilepsy" [20] research combines wavelet transforms with basic detection theory without the construction of templates. The simplicity of the method allows for nearly real-time execution.

2.4.1 Wavelet Decomposition

While wavelets can be seen as a generalization of STFT, the wavelet decomposition has many advantages over the classical STFT, such has the increase of frequency resolution in the frequency band of interest while maintaining the same time resolution (usually spike and wave

discharges are restricted to a 2.5-4.5 Hz narrow frequency window). Each EEG recording is decomposed using the Continuous Wavelet Transform (CWT) formula.

2.4.2   Sliding Variance Technique

During absence seizures, variance of the wavelet decomposed signal increases rapidly, so an algorithm is developed for the detection of absence seizures with the use of sliding windows. To avoid detecting artifacts, a double thresholding is applied, one defined by the maximum variance value during a seizure and the second one estimated from the variance between onset and offset for some known samples.

2.4.3   Conclusions

The proposed algorithm, although it doesn't need the use of an artificial network, presents an high enough accuracy degree and low false positive rates. However, its sensitivity is related to the length of the sliding window, which is to be optimized for each signal analyzed.

2.5   Artificial Neural Networks

Artificial neural network (ANN) greatly characterize the majority of the spike and wave algorithms, since they can easily adapt to every requirements that must be achieved. The study "An EEG spike detection algorithm using artificial neural network with multi-channel correlation"[21] is a prime example of using ANNs for the detection of spike and waves.
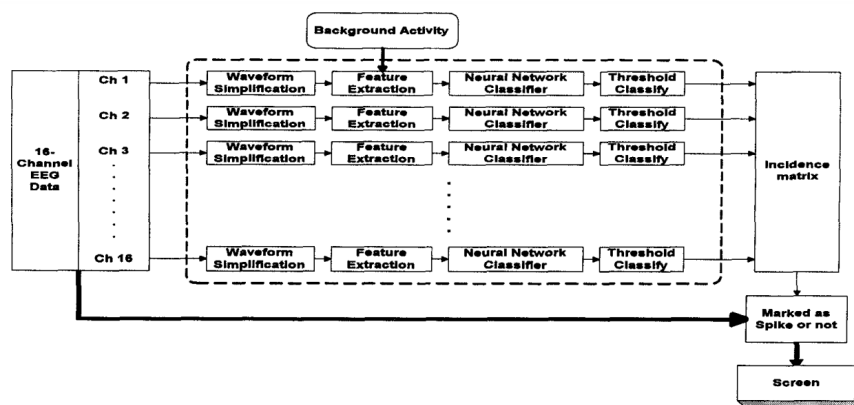
Figure 2.5.1: Detailed workflow of the artificial neural network algorithm

For the purpose of this study, radial basis function (RBF) neural network is chosen for single channel recognition, with model optimization using receiver operating characteristics analysis. Peak angle, amplitude and velocity are used as inputs for the RBF. For the classification process an optimal threshold was chosen, based on the maximization of the detection sensitivity and specificity. Finally, the concept of the incidence matrix was employed for the identification of multi-channel geometric correlation.

2.5.1 Conclusions

The sensitivity and specificity of ANNs are generally high, with a low number of false positives. However, the outputs are clearly influenced by the inputs, which can alter the outcomes and training the algorithm excessively can render it unable to process certain information.

2.6 Fuzzy Clustering

Fuzzy clustering is useful for classifying similar discontinuous temporal patterns, such as spike and wave in the EEG signals, to a set of clusters which are groups of similar waveforms. To further explore this methodology, the "Forecasting generalized epileptic seizures from the EEG signal by wavelet analysis and dynamic unsupervised fuzzy clustering"[22] study explains how this type of algorithm works.

2.6.1 Multiscale Decomposition by the Fast Wavelet Transform

The wavelet transform provides a good local representation of the signal in both the time domain and the frequency domain by looking for the spatial distribution of singularities. The wavelet transform is optimal for the EEG signals since they are non-stationary, both in time and frequency. By applying this method, features from the EEG signals are extracted

2.6.2 Unsupervised Optimal Fuzzy Clustering (UOFC) algorithm

Once the features from the EEG signals are extracted, they are inserted as inputs for the clustering procedure (or they can be reduced for a minimal computational load). The clustering is utilized for the finding of matching groups within the input features. Studying the dynamics of these nonuniform features can predict the bio-electrical brain activity. Clustering is done with UOFC[23], which divides the data with a combination of the fuzzy k-means[24] and maximum-likelihood estimation (MLE) algorithms. UOFC operates with these steps:

- Choosing of the initial cluster prototype at the mean location of all data features

- Calculation of partition of the dataset with fuzzy k-means and MLE

- Calculation of the performance measures for cluster validity

- Adding of another cluster prototype equally distant from all data features

- Choosing of optimal partition when number of clusters are bigger than a pre-decided maximum number of clusters
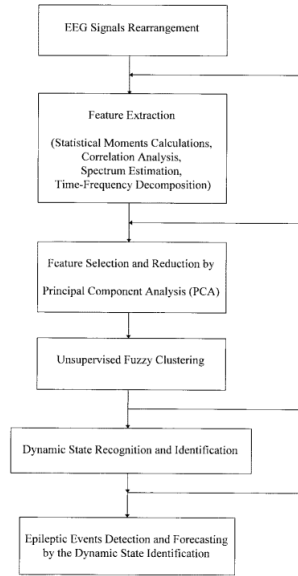
Figure 2.6.1: Detailed workflow of the fuzzy clustering algorithm

2.6.3 Conclusions

The suitability and effectiveness of this method for finding spike and waves are satisfactory, the specificity is rather good but the sensitivity is rather limited, because of the limitations of surface recordings and number electrodes.

2.7 Chaos Theory

The research "Temporal epilepsy seizures monitoring and prediction using cross-correlation and chaos theory"[25] proposes an approach which combines high correlation observation between any pair of electrodes for the lower frequencies and a decrease in the Lyapunov index (chaos or entropy) for the higher frequencies. Power spectral density and statistical analysis tools are used to determine threshold levels for the lower frequencies. The use of the Lyapunov exponent is a powerful measure to detect and characterise the behaviour of a dynamic system, which can be either chaotic or irregular. This behaviour is described through the use of non-linear differential equations. The Lyapunov exponent is mainly used for in depth analysis of local stability for stationary states in different wave trajectories.

2.7.1 Learning Process

The algorithm determines voltage thresholds for delta frequencies during pre-ictal and inter-ictal states. Highest cross correlation between electrodes is established along entropy level in the gamma subbands to compute the values and derivative of Lyapunov index.
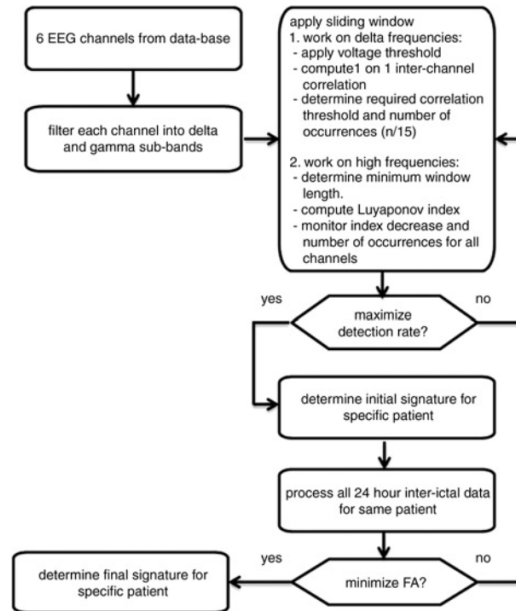
Figure 2.7.1: Detailed workflow of the chaos theory algorithm

2.7.2 Conclusions

The study showed that seizures can be anticipated by analysing delta and gamma subbands, while other subbands do not present any significant or useful information, while achieving an high enough accuracy with a low false positive rate.

2.8 Nonlinear Dynamic System Theory

The EEG signals, like many other biological phenomena, are quite likely governed by nonlinear dynamics. To uncover certain features of the underlying dynamics of these signals, nonlinear dynamic system theory is one of the main methodologies. The study "Detection of Seizures from Small Samples Using Nonlinear Dynamic System Theory"[26] uses nonlinear dynamic system theory along correlation dimension of unbiased autocovarianced EEG signals (UAD_2).

2.8.1 Nonlinear settings for EEG signal processing

In a nonlinear system many solutions eventually move toward an attractor. To correctly characterize the behavior of a nonlinear dynamic system, the geometry of the attractors must be delineated. The most commonly used mathematical technique for this task is the algorithm of Grassberger-Procaccia (GP)[27], which takes the single-variable time series, reconstructs its state-space attractor with delay-embedding and returns an estimate of the attractor's dimension. Since seizures are short-duration chaotic data, the EEG signals are preprocessed with unbiased autocovariance, which suppresses chaotic components while augmenting oscillatory ones. With

this preprocessing, the attractors have a much lower dimension. The steps can be summarized as it follows:

1. Parameter determination for UAD_2 computation: for these type of signals, a low embedding dimension is chosen along with a low delay time and a low cut-off distance for the GP algorithm

2. Threshold determination for the detection of seizures based on UAD values.

2.8.2   Conclusions

The technique proves to be computationally robust while detecting various types of seizures in near-real time. However, since it depends on the parameters of embedding dimension, delay and lag time, it can lead to false positive results.

Chapter 3

Material and Methods

3.1 Dataset

The dataset utilised for the study of EEG of epileptic patients is from CHB-MIT database[28], extracted from Physionet[29]. This database was collected at the Children's Hospital Boston and it consists of EEG recordings from pediatric subjects with intractable seizures. Subjects were monitored for up to several days following withdrawal of anti-seizure medication in order to characterize their seizures and assess their candidacy for surgical intervention.

3.1.1 Dataset's structure

This dataset consists of recordings from 23 subjects (5 males, ages 3-22; 17 females, ages 1.5-19)(Case chb21 was obtained 1.5 years after case chb01, from the same female subject, and case chb24 was added to this collection in December 2010, not currently included in the subjects' s info). Below a list of the subjects aforementioned.

Subject	Gender	Age (years)
chb01	F	11
chb02	M	11
chb03	F	14
chb04	M	22
chb05	F	7
chb06	F	1.5
chb07	F	14.5
chb08	M	3.5
chb09	F	10
chb10	M	3
chb11	F	12
chb12	F	2
chb13	F	3
chb14	F	9
chb15	M	16
chb16	F	7
chb17	F	12
chb18	F	18
chb19	F	19
chb20	F	6
chb21	F	13
chb22	F	9
chb23	F	6

Table 3.1.1: Gender and age of subjects

Each case has between 9 and 42 continuous .edf files, all of these signals are sampled at 256 Hz with 16 *bit* resolutions. Most of these files have 23 EEG signals, where each of them have the nomenclature from the international 10-20 system of EEG electrode positions, as explained in 1.3.1. In some records, other signals are added, like ECG (ElectroCardioGram) and VNS (Vagal Nerve Stimulus) signals.

3.1.2 Data Description

The dataset consists of a total of 664 .edf files, with 129 of them containing 1 or more seizures. In all, these records include 198 seizures, with the beginning and the end of each seizure annotated in .text files to facilitate the study of the epileptic EEG signals, along with the elapsed time of the recording session.
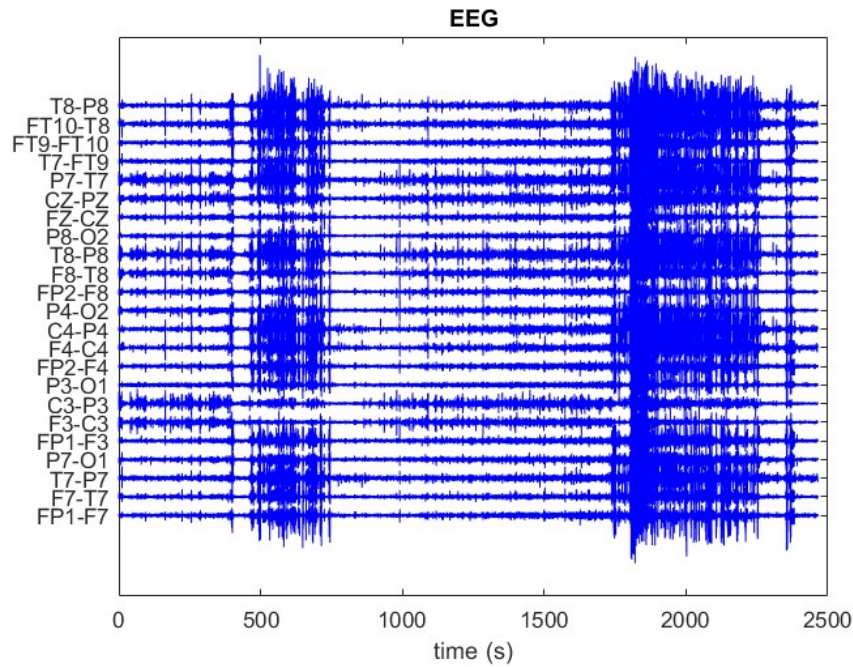
Figure 3.1.1: Example of unfiltered data from patient chb03

3.2   Preprocessing

All the analyzed signals were preprocessed before implementing the algorithm to have cleaner signals and achieve better results. The signals were filtered with a band-pass filter, obtained as a cascade of a high-pass filter with a low-pass filter. Both of these filters are IIR Chebyshev Type II filters, of order 5 and 8 respectively. The high pass filter has a cut-off frequency of 1 Hz, with the attenuation of 20 dB in the stopband at 0.75 Hz. The low pass filter has a cut-off frequency of 40 Hz, with the attenuation of 20 dB in the stopband at 44 Hz.
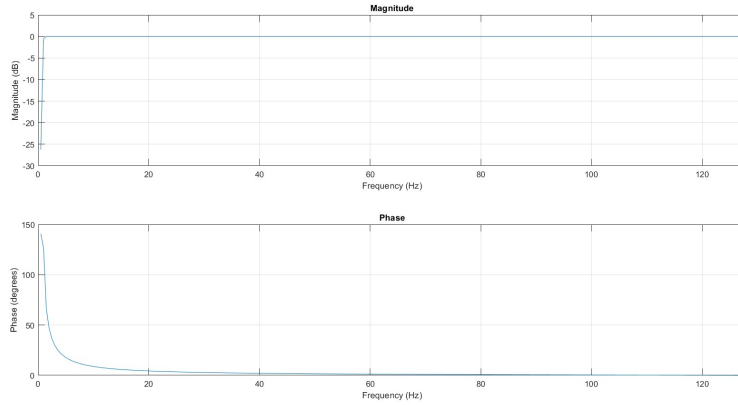
Figure 3.2.1: Bode diagram of the high-pass filter
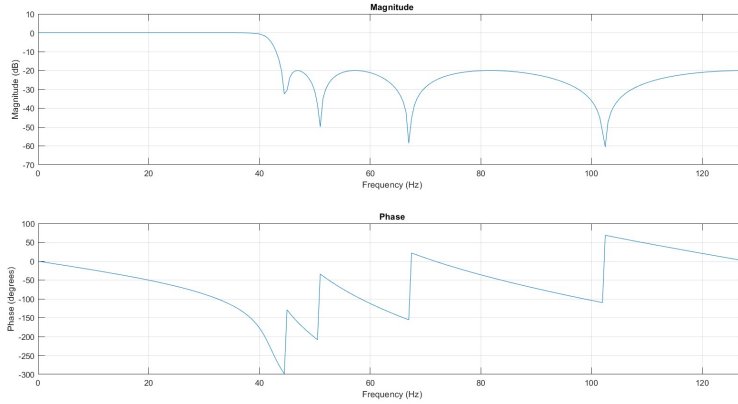
Figure 3.2.2: Bode diagram of the low-pass filter

3.2.1   EOG Artifacts Removal

For the removal of ocular artifacts, second order blind source separation is implemented with the SOBI algorithm, an automatic tool developed by German Gomez-Herrero[30].

Let $s(t)$ be the n original sources and let $x(t)$ be the m mixtures observed at the the electrodes. Let us also call Γ_{EEG} the set of indexes so that $s_i(t) \forall i \in \Gamma_{EEG}$ are the neural source potential. Likewise, Γ_{EOG} is the set of indexes so that $s_i(t) \forall i \in \Gamma_{EOG}$ are the ocular source potential. Following these labels, the signal record at j^{th} electrode can be modeled after this instantaneous mixture:

$$x_j(t) = x_{j,EEG}(t) + x_{j,EOG}(t) = \sum_{i \in \Gamma_{EEG}} (a_{ji}s_i(t)) + \sum_{i \in \Gamma_{EOG}} (a_{ji}s_i(t)) \qquad (3.2.1)$$

38

with a_{ji} being the transfer coefficient from the ith source to the jth scalp electrode. This model can be summarised by this matrix annotation:

$$x(t) = x_{EEG}(t) + x_{EOG}(t) = A(t)s(t) = A_{EEG}(t)s_{EEG}(t) + A_{EOG}(t)s_{EOG}(t) \tag{3.2.2}$$

To perform EOG correction, spatial filtering is done in these 3 steps:

1. Estimate the mixing matrix A using a window of data (usually $0.25 * m^2$ seconds)

2. Identify columns of A corresponding to EOG artifacts (sub-matrix A_{EOG}) and EEG neural components (sub-matrix A_{EEG}): such distinction can be easily done with low fractal dimension, since ocular activity have usually low-frequency components.

3. Recover the EEG activity by means of the following filter:

$$\hat{x}_{EEG}(t) = A_{EEG}A_{EEG}^{\#}x(t) \tag{3.2.3}$$

where $\#$ is the Moore-Penrose pseudoinverse[31].

3.2.2 EMG Artifacts Removal

For the removal of muscular artifacts, canonical correlation analysis (CCA) is used. As explained in section 3.2.1, the observed time can be described as:

$$x(t) = As(t) \tag{3.2.4}$$

with A as the unknown mixing matrix. The objective is to evaluate the mixing matrix to obtain the original source signal $s(t)$. To do so, the de-mixing matrix W is introduced:

$$z(t) = Wx(t) \tag{3.2.5}$$

The de-mixing matrix approximates the unknown source signals in s(t) by a scaling factor. To resolve this problem, CCA forces the sources to be mutually uncorrelated and maximally correlated with a predefined function. This predefined function $y(t)$ is a temporally delayed version of $x(t)$, to enforce the sources to be maximally correlated:

$$y(t) = x(t - 1) \tag{3.2.6}$$

After removing the mean of each row of $x(t)$ and $y(t)$, CCA obtains two sets of basis vectors to maximize the correlation of the variables projected onto these basis. Considering the linear combination of the components in $x(t)$ and $y(t)$:

$$
\begin{aligned}
x &= w_{x_1}x_1 + \cdots + w_{x_n}x_n = w_x{}^T x \\
y &= w_{y_1}y_1 + \cdots + y_{y_n}y_n = w_y{}^T y
\end{aligned}
\tag{3.2.7}
$$

CCA maximizes the correlation between $x(t)$ and $y(t)$ by solving the following problem:

$$
\begin{aligned}
\max_{w_x, w_y} \rho(x, y) &= \frac{E[xy]}{\sqrt{E[x^2]E[y^2]}} \\
&= \frac{E[(w_x{}^T x)(w_y{}^T y)]}{\sqrt{E[(w_x{}^T x)]E[(w_y{}^T y)(w_y{}^T y)]}} \\
&= \frac{w_x{}^T C_{xy} w_y}{\sqrt{(w_x{}^T C_{xx} w_x)(w_y{}^T C_{yy} w_y)}}
\end{aligned}
\tag{3.2.8}
$$

where C_{xx} and C_{yy} are the within-set covariance matrices of $x(t)$ and $y(t)$ respectively, while C_{xy} is the between-sets covariance matrix. The solution for this problem is the following one:

$$\begin{cases} C_{xx}^{-1}C_{xy}C_{yy}^{-1}C_{yx}\hat{w}_x = \rho^2\hat{w}_x \\ C_{yy}^{-1}C_{yx}C_{xx}^{-1}C_{xy}\hat{w}_y = \rho^2\hat{w}_y \end{cases}$$

The n estimates of the sources $s_i(t)$ are equal to $z_i(t) = \hat{w}_{x_i}^T x(t)$.
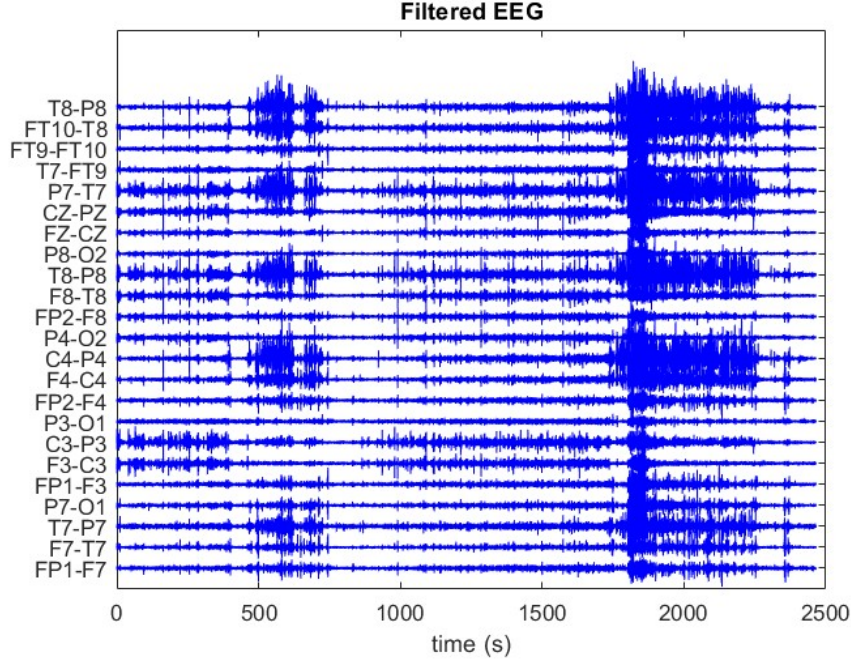
Figure 3.2.3: Example of filtered data from patient chb03

3.2.3 Noisy Signals Removal

Before the elaboration of the signals could begin, the EEG data is visually evaluated to ensure the quality of the algorithm's results. By doing this, some signals are deemed unnecessary because of their low SNR, which could trick the algorithm in finding false spike and wave patterns. To avoid these occurrences, an automatic threshold is designed based on the preprocessed signal's envelope. To calculate the signal's envelope, the preprocessed signal is rectified and then filtered with a IIR Chebyshev Type II low-pass filter of order 4. The low-pass filter has a cut-off frequency of 1 Hz, with the attenuation of 20 dB in the stop band at 1.5 Hz. Once the signal envelope $e(t)$ is obtained, the following threshold is calculated using the portion of the envelope which represents the inter-ictal and pre-ictal intervals:

$$t = \frac{\overline{e(t)} + 3 * \sigma(e(t))}{max(e(t))} \quad \sigma = \text{standard deviation; } \overline{e(t)} = \text{envelope mean} \tag{3.2.9}$$

40
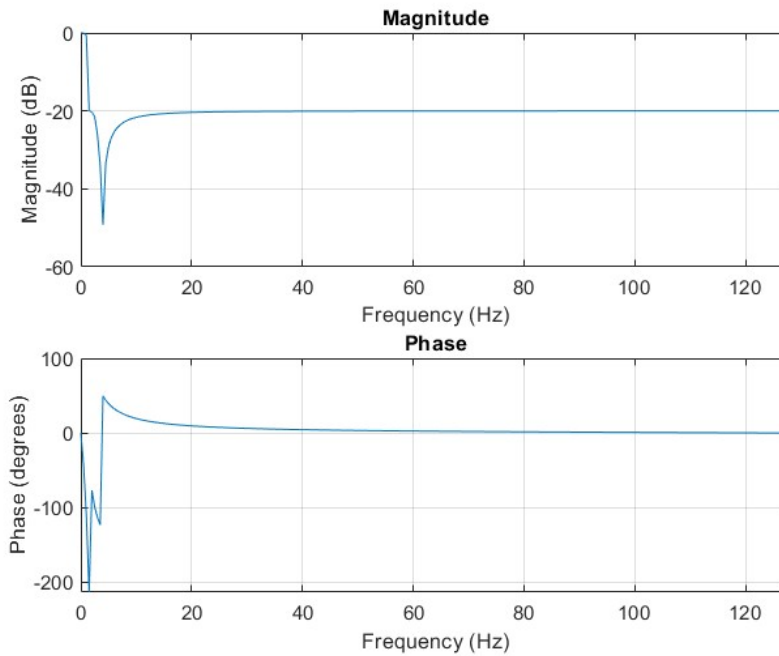
Figure 3.2.4: Bode diagram of the low pass filter

This quantity is calculated since the signals become visually less stationary when the incoming seizure is near, but with noise signals are so stationary that it's very difficult to distinguish the non-ictal intervals from the ictal interval. Signal envelopes that have a t value higher than 0.7 are discarded. Because of this operation, all the signals of chb14 are scrapped.

3.3   Algorithm

Once the signals have been preprocessed enough to not interfere with the results, it is possible to apply the algorithm by following these three steps:

1. Construction of prototypes waveforms that best represent pathological waves

2. Calculation of match filters through normalized cross-correlation, between each prototypes and each signal's channels

3. From the waves obtained in the previous step, waves that are smaller than a noise threshold are eliminated

The algorithm is implemented on MATLAB.

3.3.1 Prototypes' Construction

To obtain the waveforms that would be used for the identification of spike and wave in epileptic EEG signals, a set of 17 prototypes was handed. To obtain this set, spike and waves identified by a neurologist were given and then fitted to find a mathematical model able to describe them (a sinc function was chosen to model the spike and a gaussian function to model the wave after the spike). Thanks to these waveforms, spike and waves of an EEG signal that had a correlation high enough with these prototypes were identified.
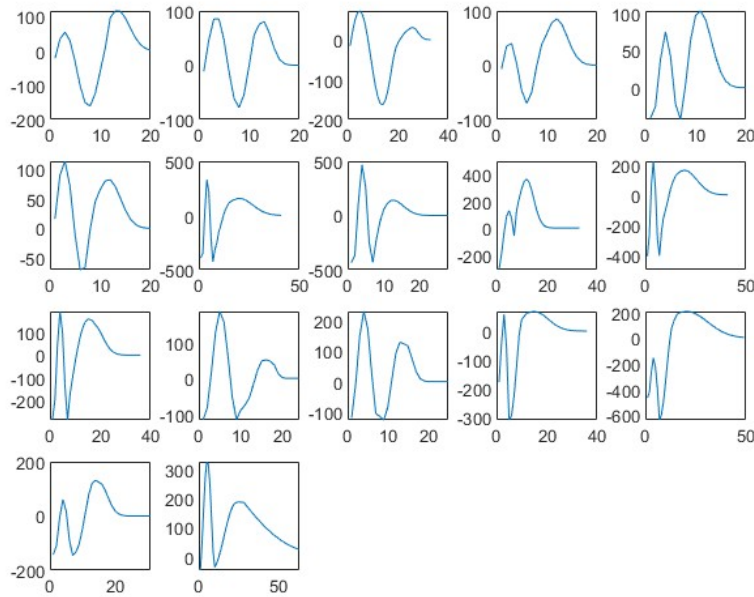
Figure 3.3.1: Old set of prototypes

To widen the range of the spike and waves that could be identified, all the intermediate waveforms of these prototypes are calculated. To do so, principal component analysis [32] is fundamental. Principal Component Analysis (PCA) is a mathematical technique used to simplify complex datasets. It identifies the most important patterns in data by finding new variables, called principal components, which capture the most significant information. It works by calculating the covariance matrix of the data, finding its eigenvalues and eigenvectors, and then transforming the data into a new space defined by the principal components. Before the following procedure, only the waveforms that have a maximum of 0.85 correlation with each other are kept to not have redundant information. By doing this, only 12 of the initial 17 prototypes are kept. Assuming as X the matrix containing the prototypes, where each column is a waveform:

$$X = \begin{pmatrix} X_1 \\ X_2 \\ \vdots \\ X_n \end{pmatrix} = \begin{pmatrix} X_{11} & X_{12} & \cdots & X_{1n} \\ X_{21} & X_{22} & \cdots & X_{2n} \\ \vdots & \vdots & \ddots & \vdots \\ X_{l1} & X_{l2} & \cdots & X_{ln} \end{pmatrix} \text{ with } i = 1, 2, ..., n \text{ and } j = 1, 2, ..., l \quad (3.3.1)$$

Given this matrix, these steps are followed:

1. **Standardization**
   For this step, each value of each variable is subtracted the mean and divided by the standard deviation:

$$z = \frac{X_i - \mu}{\sigma} \quad (3.3.2)$$

2. **Covariance matrix computation**
   The covariance matrix $Cov(X, Y)$ of the whole dataset is computed:

$$Cov(X, Y) = \frac{1}{n} \sum_{i=1}^{n} (x - \bar{x})(y - \bar{y}) \quad (3.3.3)$$

3. **Calculation of eigenvalues and eigenvectors**
   An eigenvector is a nonzero vector that changes at most by a scalar factor when that linear transformation is applied to it. The corresponding eigenvalue is the factor by which the eigenvector is scaled. To calculate them, the following equations are applied:

$$\begin{aligned} Cov(X, Y)v &= \lambda v \\ Cov(X, Y)v - \lambda v &= 0 \\ (Cov(X, Y) - \lambda I)v &= 0 \end{aligned} \quad (3.3.4)$$

Since v is a non-zero vector, the only way this equation can be equal to zero is:

$$det(Cov(X, Y) - \lambda I) = 0 \quad (3.3.5)$$

4. **Sort eigenvalues and their corresponding eigenvectors**

5. **Pick k eigenvalues and form a matrix of eigenvectors**

This transformation retains as much relevant information as possible while reducing the number of variables. For the purpose of this study, the first 3 eigenvectors are retained, since they contain the great majority of the information of the set of prototypes (so a $n \ x \ 3$ matrix is obtained). Once we have the matrix, the convex hull is calculated[33] so that we can obtain a more uniformed space of intermediate points. The next step is to apply a FEM (finite element method[34]) mesh algorithm to find every possible point in the convex hull. After this operation, the next procedure is to convert the m points of the meshed convex hull into waveforms by
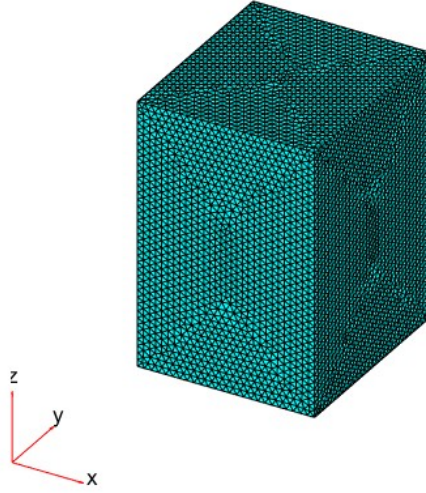
Figure 3.3.2: Meshed convex hull

multiplying the matrix of points P ($n \ x \ 3$ matrix) to the matrix of the **scores** S ($l \ x \ 3$ matrix), the representations of the matrix X in the principal component space:

$$Y = \begin{pmatrix} Y_{11} & Y_{12} & \cdots & Y_{1m} \\ Y_{21} & Y_{22} & \cdots & Y_{2m} \\ \vdots & \vdots & \ddots & \vdots \\ Y_{l1} & Y_{l2} & \cdots & Y_{lm} \end{pmatrix} = \begin{pmatrix} S_{11} & \cdots & S_{1k} \\ S_{21} & \cdots & S_{2k} \\ \vdots & \ddots & \vdots \\ S_{l1} & \cdots & S_{lk} \end{pmatrix} \cdot \begin{pmatrix} P_{11} & P_{12} & \cdots & P_{1m} \\ \vdots & \vdots & \ddots & \vdots \\ P_{k1} & P_{k2} & \cdots & P_{km} \end{pmatrix} \tag{3.3.6}$$

con $k=3$

with Y the matrix of the possible intermediate prototypes. For the final step, we filter the intermediate waveforms so that the remaining ones only have a maximum of *0.85* correlation between each other, and a smoothing with the combination of two *tukeywin* windows is applied, so that the remaining waveforms begin and finish at 0 (a further correlation filtering as the one aforementioned is applied again).
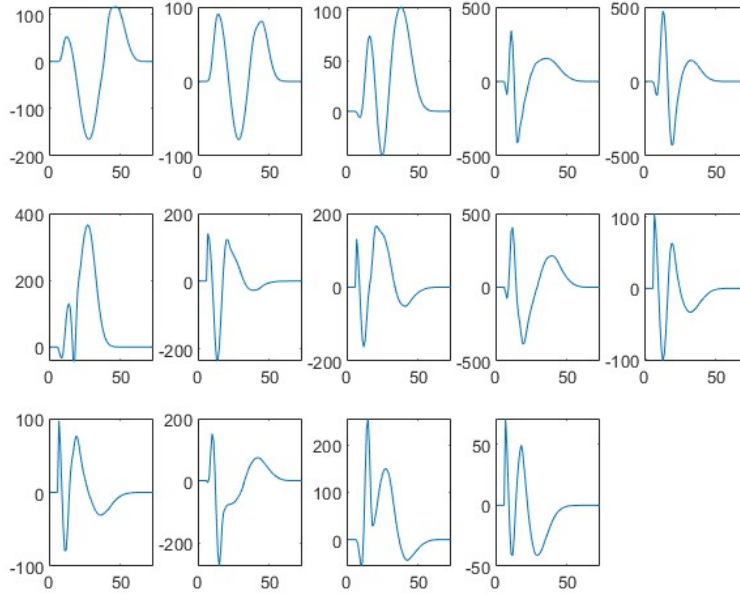
Figure 3.3.3: New set of prototypes

3.3.2   Match Filtering

To compare the new set of prototypes with the preprocessed data, a matched filter is applied [35]. In short, what a matched filter does is to identify a piece of signal, although covered by noise, with a prototype signal. To achieve this result, the known signal is correlated with the unknown signal by making the convolution between the unknown signal and the time-reversed known signal. This technique also maximizes the signal-to-noise ratio (SNR) when the signal is corrupted by stochastic noise.

Considering a general signal $s(t)$ added with white noise $n(t)$, the filter, which is the time reversed of the input signal and maximizes the SNR, is $h(t)$, and the output signal is $y(t)$.

Figure 3.3.4: Filter structure

The SNR is given by the following equation:

$$SNR(T) = \frac{|\int_0^T h(\tau)y(T-\tau)\,d\tau|^2}{\sigma^2 \int_0^T |h(\tau)|^2\,d\tau}\text{with } \sigma^2 = \text{noise variance} \qquad (3.3.7)$$

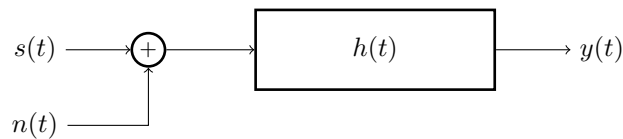To obtain the matched filter signal $y_{MF}(t)$, the signal output $y(t)$ is filtered with the time reversed filter $h(t)$:

$$y_{MF}(t) = y(t) * h(-t) = \int_{-\infty}^{\infty} y(t)h(t-T)\,dt \qquad (3.3.8)$$

This method equals to a normalized cross-correlation with a signal and a conjugated time-reversed template.

Match filters are highly effective if the known waveform is precisely know, leading to optimal results with low computational complexity. Nonetheless, it is very sensitive to changes with the object. This filter is used to identify the shapes of the prototypes within the signal, even if there is some noise.If a certain threshold is reached, it signifies that both signal match[36].

3.3.3 Calculation of Normalized Cross-Correlation

To apply the match filter with the set of prototypes and the signals, the following normalized cross-correlation was computed:

$$C(t) = \frac{\int x(\tau)w(t+\tau)d\tau}{||x||_2||w||_2} \qquad (3.3.9)$$

The EEG channel is $x(t)$, while the prototype waveform is $w(t)$ and $||.||_2$ is the root mean square (RMS) of the argument. The cross-correlation (which is the numerator in the equation 3.3.9) is divided by the energy of the portion of the signal and of the prototype.

Due to this normalization, the cross-correlation values vary between -1 and 1. A value equal to -1 means that the portion of the signal matches perfectly with time reversed prototype. On the other hand, a value equal to 1 means that the portion of the signal matches perfectly with the prototype. The choice to normalize the cross-correlation is made to identify signals which morphology matches the prototypes, even though their amplitude are not the same.

While the prototypes were based on real spike-and-waves, a value of -1 or 1 can never be obtained since they were fitted on mathematical models and because of noise within the signal. Because of these reasons, a threshold was applied to determine if a portion of a signal matches with the prototype. At first, it was decided to use an absolute normalized cross-correlation threshold of 0.85, but it was deemed not optimal since many spike-and-waves were clearly not detected. Therefore, a variable threshold is applied, based on the percentiles of the normalized cross-correlation values. The percentile are calculated from 0 to 100 with a 0.1 step and the percentile closest to 0.85 is selected, greatly increasing the number of spike and waves found in the signals.

Examples of waveforms identified by the algorithm are shown below. The detected spike and waves are shown in red, including all the channels in which the spike and waves are noted.
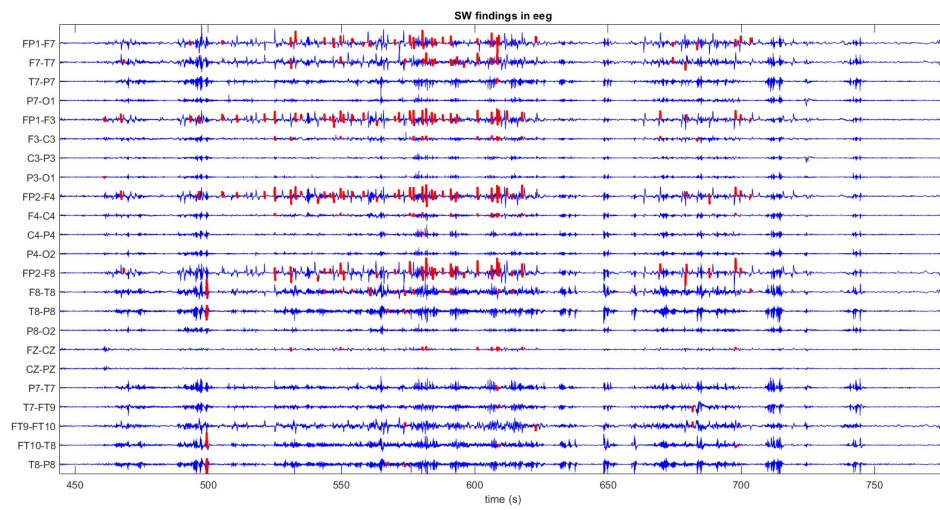
Figure 3.3.5: Waveforms identified in 5 minutes of chb03's EEG signal

Chapter 4

Results

4.1 Evaluation of Algorithm's results

To evaluate the obtained results, the frequency of spike and waves discharges (SWD) was calculated based on the found spike and waves. All detected SWs of every single EEG channel are considered simultaneously, while discarding SWs that are ascertained in multiple channels: every validated SW has a minimum distance from one another of 5 samples, equal to 19 ms. By doing this, a vector defined as $firing(t)$ is obtained, which is as long as a single EEG channel of the examined EEG recording, containing every single instance of detected SW. Once this vector is obtained, the frequency $F(t)$ of the SWD is computed with this equation:

$$F(t) = \frac{\int firing(\tau)o(t+\tau)d\tau}{60} \tag{4.1.1}$$

with $o(t)$ a vector of ones with a length equal to 60 s of samples. By applying this formula, the mean frequency of SWD in epochs of 60 s is calculated for all epileptic signals. An example is shown in the figure below, representing the mean frequencies for each EEG seizure recording of the patient chb18:
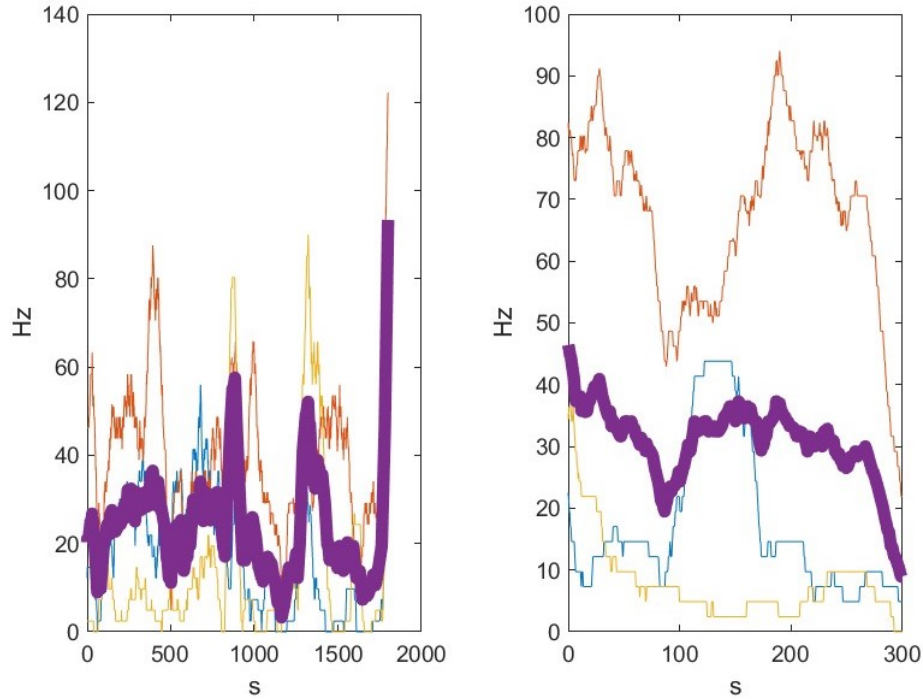
Figure 4.1.1: Mean frequency plot of chb18: in the left one, the mean frequency plot of 30 minutes before the seizure events; in the right one one, the mean frequency plot of 5 minutes after the seizure event

While a good majority of the computed frequencies shows that the spike and wave's frequency discharge grows as soon as the seizure is coming, there are also cases which prove the opposite, in other cases the frequency shows a stochastic trend (like in the figure shown below). This means that, while the frequency discharge of the spike and waves is good indicator of an incoming seizure, it's not a sufficiently reliable one.
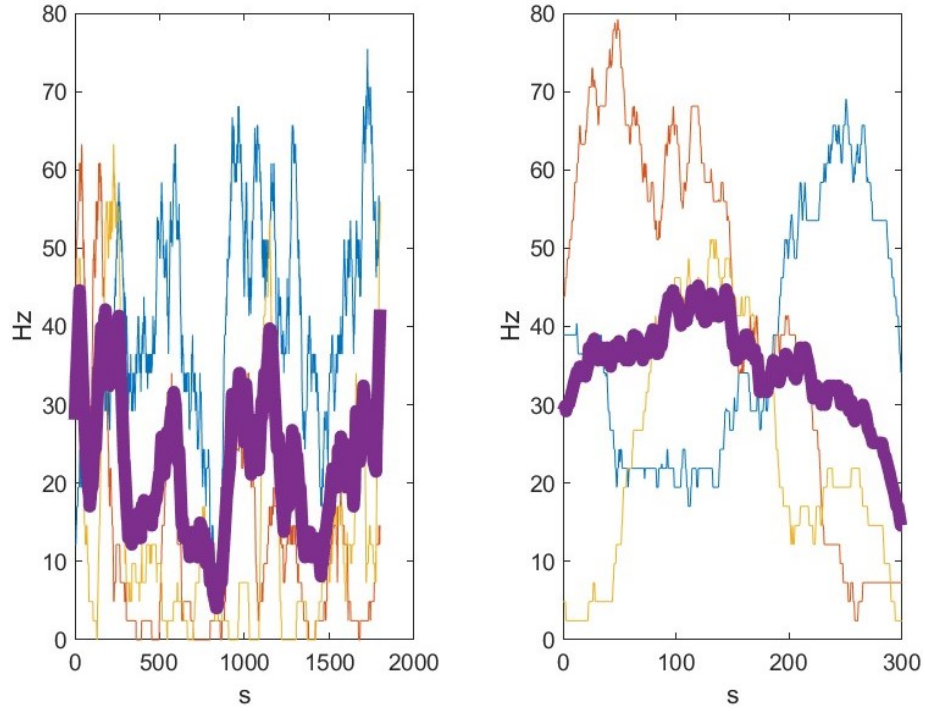
Figure 4.1.2: Mean frequency plot of chb13

Another feature extracted from the detected spike and waves is their amplitude, calculated with the root mean square (RMS), which is defined as:

$$RMS = \sqrt{\frac{\sum_{i=1}^{N} x_i{}^2}{N}} \tag{4.1.2}$$

To resume these first results, the following boxing plots represent the mean number of detected spike and waves and their amplitude during the inter-ictal, the pre-ictal and the post-ictal period.

Figure 4.1.3: Number of identified spike and waves

Figure 4.1.4: Amplitude of identified spike and waves

The Wilcoxon signed-rank test is applied to test the significant differences between these two features in each period. For the number of identified spike and waves, values of the ranking test differed between a minimum of 0.3726 and a maximum of 0.7074, which don't demonstrate a high statistical difference between the numb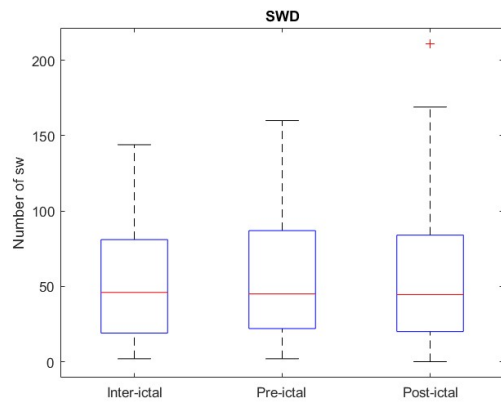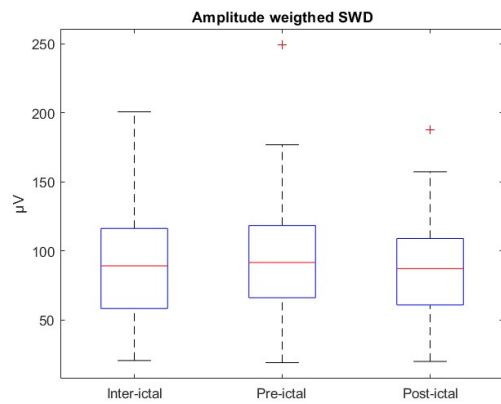er of spike and waves in each period. For the amplitude of the identified spike and waves, values are lower than 0.06, with a value of 0.0279 obtained by comparing the inter-ictal period with the pre-ictal period, which can help in order to predict the seizure.

	Wilcoxon signed-rank test		
Type of feature analyzed	Intra-ictal period vs Pre-ictal period	Pre-ictal period vs Post-ictal period	Inter-ictal period vs Post-ictal period
Number of spike and waves	0.5339	0.3726	0.7074
Amplitude of spike and waves	0.0279	0.0008	0.0515

Table 4.1.1: Wilcoxon signed-rank test results

4.2 Machine Learning

To further explore the obtained results, other features from the detected spike and waves are extracted: alongside the number of SW, their amplitude and frequency discharge, the standard deviation and the gradient of the frequency discharge are also computed. These features are obtained from dividing the interval of 30 minutes before the seizure into 5 minutes epochs, which overlap between them by 1 minute. An example of the results of doing so are shown in the figure below.
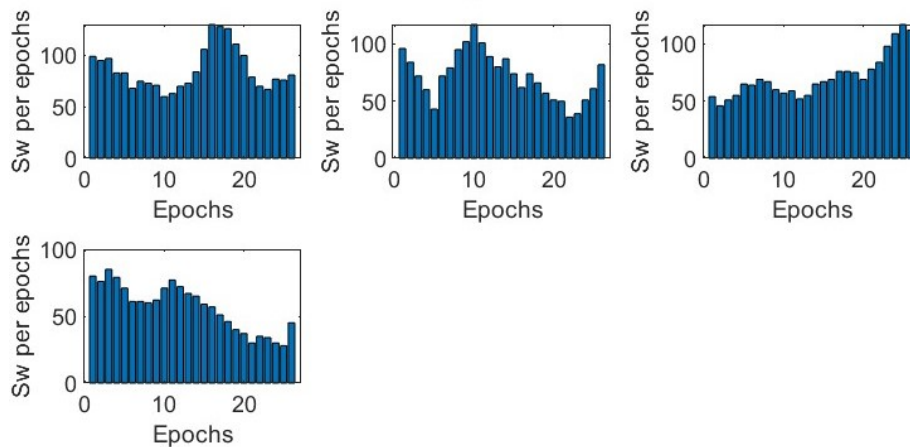

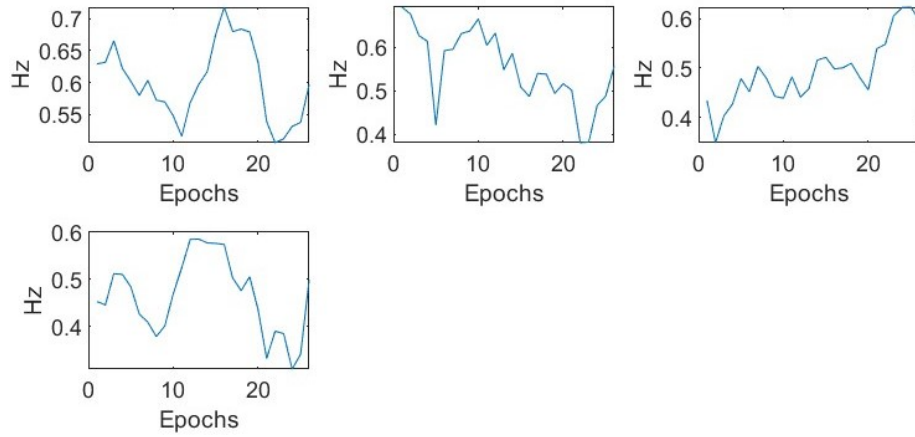Figure 4.2.1: Number of detected SWs per epochs in chb08

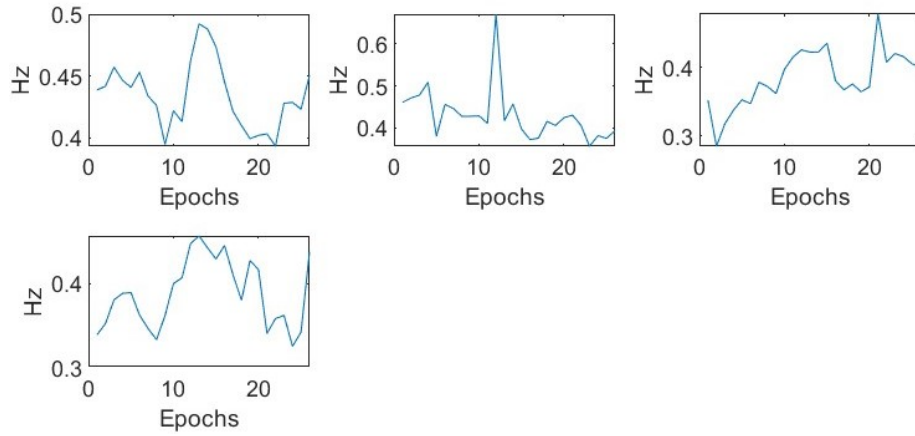Figure 4.2.2: Frequency discharge of detected SWs in chb08

Figure 4.2.3: Standard deviation of frequency discharge of detected SWs in chb08
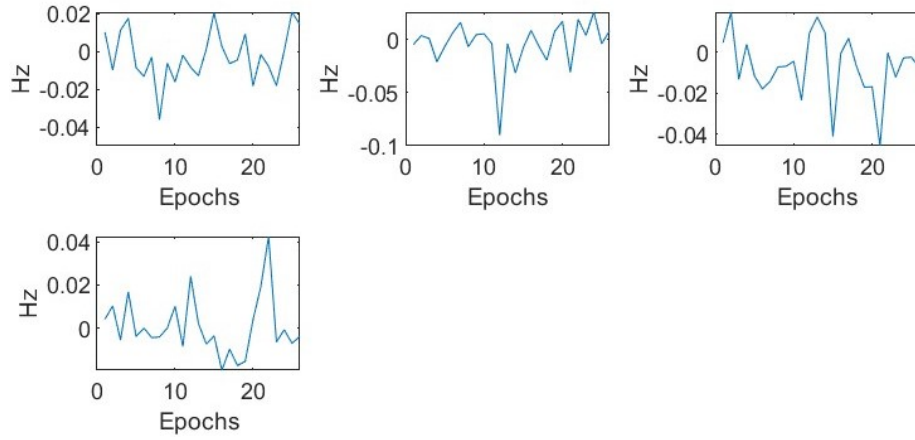
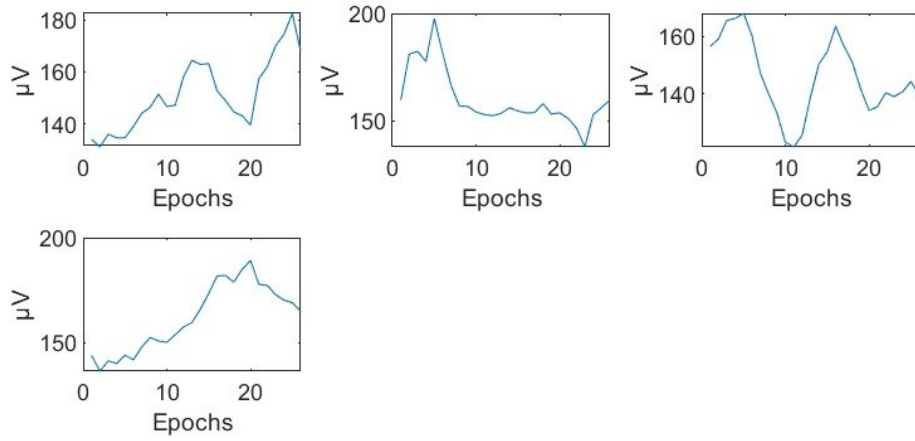Figure 4.2.4: Gradient of frequency discharge of detected SWs in chb08

Figure 4.2.5: Amplitude of detected SWs in chb08

Once these features are computed, the first 5 epochs of each feature are extracted and classified them as the inter-ictal time interval, corresponding to an interval of 30 to 20 minutes before the seizure. A similar approach is used for the last 5 epochs of each feature, corresponding to an interval of 10 to 0 minutes before the seizure, therefore being classified as the pre-ictal time interval. After this operation, MATLAB's classification learners are used to train the algorithms on these features to predict the oncoming attack. For this purpose, 10 % of these epochs are used as test data, while the remaining percentage is used to train and validate the classifiers. The cross-validation is used as a validation scheme to protect the algorithm from over-fitting. Below a table of the best trained classifiers of each family and their validation accuracy.

Classifiers' validation accuracy		
Classifier	Classifier's family	Accuracy (Validation)
Medium Tree	Decision trees	59.4%
Quadratic Discriminant	Discriminant Analysis	47.6%
Binary GLM Logistic Regression	Logistic Regression Classifiers	43.3%
Kernel Naive Bayes	Naive Bayes Classifiers	53.8%
Fine Gaussian SVM	Support Vector Machine	67.1%
Efficiently Linear SVM	Efficiently Trained Linear Classifiers	46.0%
Weighted KNN	Nearest Neighbour Classifiers	68.5%
SVM Kernel	Kernel Approximation Classifiers	60.5%
Bagged Trees	Ensemble Classifiers	64.4%
Wide Neural Network	Neural Network Classifiers	63.5%

Table 4.2.1: Trained Classifiers' validation accuracy

These values represent the ability of the classifiers to identify inter-ictal and pre-ictal intervals based on the given features.While these values can change for each training session, the best classifier remains the weighted K Nearest Neighbours (KNN), with an accuracy value on the test set of 70.5%. To summarize the classifier's results, the following variables are defined:

- **True positive (TP)**: the epochs that are labeled as pre-ictal are correctly classified

- **True negative (TN)**: the epochs that are labeled as inter-ictal are correctly classified

- **False positive (FP)**: the epochs that are labeled as inter-ictal are incorrectly classified as pre-ictal

- **False Negative (FN)**: the epochs that are labeled as pre-ictal are incorrectly classified as inter-ictal

By using these variables, the following measures to evaluate the classifier's results are computed:

- **Sensitivity or True Positive Rate (TPR)**

$$TPR = \frac{TP}{TP + FN} \qquad (4.2.1)$$

which is a measure of the classifier's ability to correctly identify the given epochs with the ratio between the true positives and the sum of the true positives with the false negatives

- **Precision or Positive Predictive Value (PPV)**

$$PPV = \frac{TP}{TP + FP} \tag{4.2.2}$$

which determines the probability that an epoch identified as pre-ictal is correctly guessed

- **Miss rate or False Negative Rate (FNR)**

$$FNR = \frac{FN}{FN + TP} \tag{4.2.3}$$

which is a performance metric that measures the probability that the classifiers predicts negative when the true value is positive.

- **False Discovery Rate (FDR)**

$$FDR = \frac{FP}{FP + TP} \tag{4.2.4}$$

which defines the probability that the classifiers detects false positives out of the total positives

The values of these parameters are shown in the figures below.
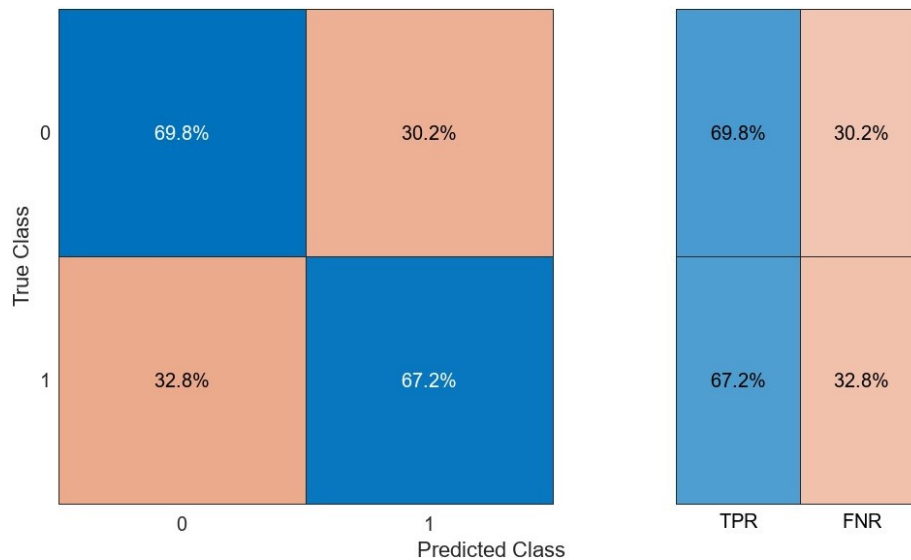
Figure 4.2.6: TPR and FNR of the weighted KNN classifier
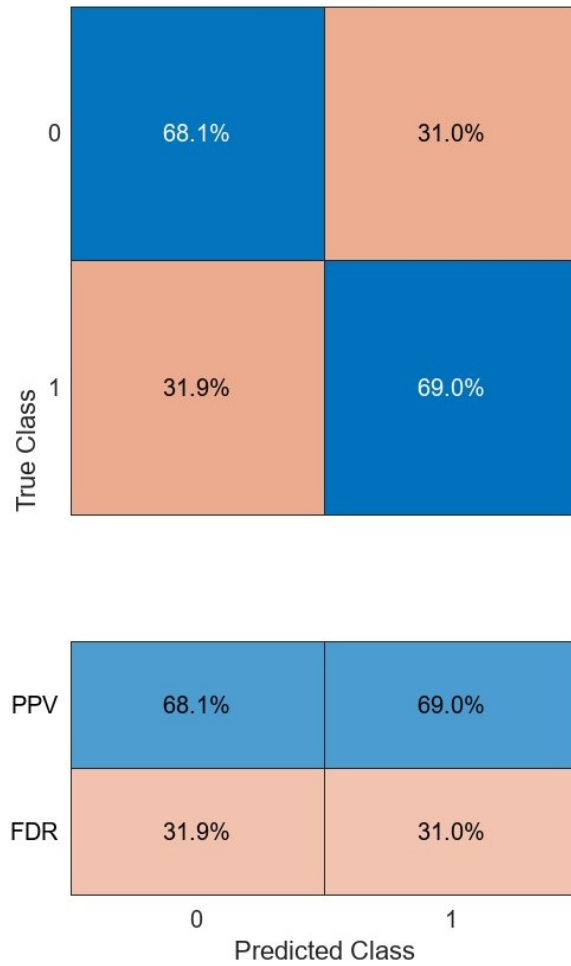
Figure 4.2.7: PPV and FDR of the weighted KNN classifier

The tables show that the features extracted from the detected SWs can allow us to distinguish the pre-ictal features from the intra-ictal features, meaning that the incoming seizure can be predicted based on the SWs, but the accuracy is not high enough to allow us to make a predictive statement. The use of other SW's features, like PSD, could help us in the prediction of the incoming epileptic attack.

Chapter 5

Conclusions and Future Works

The identification of spike and waves in patients suffering from epilepsy is important for the medical evaluation and therapy, so the development of an automatic tool is useful to optimize and support the work of neurologists. In particular, the EEG signals regarding these pathological events have an extensive duration, especially when recording asleep epileptic patients, so a simple automatic algorithm that can analyse hours of signal in few minutes is required.

In this study a fast and accurate method is introduced, capable of being used in real-time, able to identify spike and waves with the use of matching prototypes and normalized cross-correlation. While the method is fast, it's also prototype-dependent, so that's why all the intermediate prototypes are computed, while keeping the ones that are enough different from one another to avoid redundant results. By computing all the intermediate signals from the initial batch of prototypes, a greater number of spike and waves is obtained from the signals, compared to the number of the spike and waves identified by the initial set of prototypes. But even doing so can be insufficient, since the method works on the shape of the signal: signals with low SNR can present altered shapes, making the algorithm detect false spike and waves and missing real spike and waves that are too deformed to be recognized. While an adaptive and noise thresholds have been introduced to find as many real spikes and waves as possible, these methods are not perfect and it can affect the obtained results. It's also important to note that the set of prototypes was obtained by bipolar signals and are tested on the same type of signals, so using this method on monopolar signals can lead to inaccurate conclusions. Monopolar setups with average references are especially problematic since the shape of the spike and waves differ from bipolar setups. Another improvement can be done on the preprocessing of the EEG recording: while the great majority of the signals are preprocessed efficiently, there are some recordings that had to be discarded because of insufficient filtering. One last improvement can be done on the type of prototypes used for match filtering: instead of using as many diverse prototypes as possible, it could be achievable to determine the spike and waves which are majorly present in the patient's EEG recordings and compute the intermediate spike and waves associated with the patient, making the spike and wave detection patient based.

Despite these shortcomings, the results and the literature show us that there is a factor which determines the arrival of the epileptic attack. While the frequency discharge present itself as stochastic, our best results reveal that the amplitude of the spike and wave is important to

consider, since the good majority of the detected spike and waves emerge, amplitude-wise, from the normal EEG electrical activity when the seizure is approaching. Future studies could focus on the extraction of other spike and wave's features from inter-ictal and pre-ictal periods, allowing allow us to better understand the dynamics behind the seizure events. Future analysis can also be done with spikes instead of spike and waves, as noted in [37], which states a predictive model based on the number of spikes detected in the recorded EEG signals. One last suggestion is that this study focused on the comprehension of the spike and waves while considering all the brain regions, so a future study could be done on the understanding of the spike and wave based on the single recorded brain regions. There are many more possibilities to explore regarding the subject of spike and waves, all to improve people's healthspan.

Bibliography

[1]   J Gordon Betts et al. "Anatomy & physiology.(2013)". In: *Open Stax College* 1.1 (2013), pp. 1–1.

[2]   John Nolte. *The human brain*. Mosby/Elsevier, 1993.

[3]   Shane A Liddelow. "Fluids and barriers of the CNS: a historical viewpoint". In: *Fluids and Barriers of the CNS* 8 (2011), pp. 1–17.

[4]   Chet C Sherwood and Aida Gómez-Robles. "Brain plasticity and human evolution". In: *annual review of anthropology* 46 (2017), pp. 399–419.

[5]   Oluwatobi Ariyo and Farhana Akter. "Anatomy and Physiology of the Neuron". In: *Neuroscience for Neurosurgeons* (2023), p. 72.

[6]   Mark W Barnett and Philip M Larkman. "The action potential". In: *Practical neurology* 7.3 (2007), pp. 192–197.

[7]   Ettore Beghi. "The epidemiology of epilepsy". In: *Neuroepidemiology* 54.2 (2020), pp. 185–191.

[8]   James J Riviello Jr. "Classification of seizures and epilepsy". In: *Current neurology and neuroscience reports* 3.4 (2003), pp. 325–331.

[9]   Simon Shorvon, Emilio Perucca, and Jerome Engel Jr. *The treatment of epilepsy*. John Wiley & Sons, 2015.

[10]   Katarzyna Blinowska and Piotr Durka. "Electroencephalography (eeg)". In: *Wiley encyclopedia of biomedical engineering* (2006).

[11]   Hal Blumenfeld. "Cellular and network mechanisms of spike-wave seizures". In: *Epilepsia* 46 (2005), pp. 21–33.

[12]   Tiejia Jiang et al. "Improved Spike Detection Algorithm Based on Multi-Template Matching and Feature Extraction". In: *IEEE Transactions on Circuits and Systems II: Express Briefs* 69.1 (2022), pp. 249–253. DOI: 10.1109/TCSII.2021.3092141.

[13]   Romila Mushtaq and Anne C Van Cott. "Benign EEG variants". In: *American journal of electroneurodiagnostic technology* 45.2 (2005), pp. 88–101.

[14]   Themis P Exarchos et al. "EEG transient event detection and classification using association rules". In: *IEEE Transactions on Information Technology in Biomedicine* 10.3 (2006), pp. 451–457.

[15] Rakesh Agrawal, Ramakrishnan Srikant, et al. "Fast algorithms for mining association rules". In: *Proc. 20th int. conf. very large data bases, VLDB*. Vol. 1215. Santiago, Chile. 1994, pp. 487–499.

[16] Ravi Kothari and Dax Pitts. "On finding the number of clusters". In: *Pattern Recognition Letters* 20.4 (1999), pp. 405–416.

[17] Usama M Fayyad and Keki B Irani. "Multi-interval discretization of continuous-valued attributes for classification learning". In: *Ijcai*. Vol. 93. 2. 1993, pp. 1022–1029.

[18] Alexandros T Tzallas, Markos G Tsipouras, and Dimitrios I Fotiadis. "The use of time-frequency distributions for epileptic seizure detection in EEG recordings". In: *2007 29th Annual International Conference of the IEEE Engineering in Medicine and Biology Society*. IEEE. 2007, pp. 3–6.

[19] François Auger and Éric Chassande-Mottin. "Quadratic Time-Frequency Analysis I: Cohen's Class". In: *Time-Frequency Analysis: Concepts and Methods* (2008), pp. 131–163.

[20] Petros Xanthopoulos et al. "A novel wavelet based algorithm for spike and wave detection in absence epilepsy". In: *2010 IEEE International Conference on BioInformatics and BioEngineering*. IEEE. 2010, pp. 14–19.

[21] Cheng-Wen Ko et al. "An EEG spike detection algorithm using artificial neural network with multi-channel correlation". In: *Proceedings of the 20th Annual International Conference of the IEEE Engineering in Medicine and Biology Society. Vol. 20 Biomedical Engineering Towards the Year 2000 and Beyond (Cat. No. 98CH36286)*. Vol. 4. IEEE. 1998, pp. 2070–2073.

[22] Amir B Geva and Dan H Kerem. "Forecasting generalized epileptic seizures from the EEG signal by wavelet analysis and dynamic unsupervised fuzzy clustering". In: *IEEE Transactions on Biomedical Engineering* 45.10 (1998), pp. 1205–1216.

[23] Isak Gath and Amir B. Geva. "Unsupervised optimal fuzzy clustering". In: *IEEE Transactions on pattern analysis and machine intelligence* 11.7 (1989), pp. 773–780.

[24] James C Bezdek. *Pattern recognition with fuzzy objective function algorithms*. Springer Science & Business Media, 2013.

[25] Tahar Haddad et al. "Temporal epilepsy seizures monitoring and prediction using cross-correlation and chaos theory". In: *Healthcare technology letters* 1.1 (2014), pp. 45–50.

[26] Ilker Yaylali, Hüseyin Koçak, and Prasanna Jayakar. "Detection of seizures from small samples using nonlinear dynamic system theory". In: *IEEE Transactions on Biomedical Engineering* 43.7 (1996), pp. 743–751.

[27] J-P Eckmann and David Ruelle. "Fundamental limitations for estimating dimensions and Lyapunov exponents in dynamical systems". In: *Physica D: Nonlinear Phenomena* 56.2-3 (1992), pp. 185–187.

[28] J Prasanna et al. "Automated epileptic seizure detection in pediatric subjects of CHB-MIT EEG database—a survey". In: *Journal of Personalized Medicine* 11.10 (2021), p. 1028.

[29] George B Moody. "PhysioNet". In: *Encyclopedia of Computational Neuroscience*. Springer, 2022, pp. 2806–2808.

[30] Germán Gómez-Herrero et al. "Automatic removal of ocular artifacts in the EEG without an EOG reference channel". In: *Proceedings of the 7th Nordic signal processing symposium-NORSIG 2006*. IEEE. 2006, pp. 130–133.

[31] João Carlos Alves Barata and Mahir Saleh Hussein. "The Moore–Penrose pseudoinverse: A tutorial review of the theory". In: *Brazilian Journal of Physics* 42 (2012), pp. 146–165.

[32] Takio Kurita. "Principal component analysis (PCA)". In: *Computer Vision: A Reference Guide* (2019), pp. 1–4.

[33] Raimund Seidel. "Convex hull computations". In: *Handbook of discrete and computational geometry*. Chapman and Hall/CRC, 2017, pp. 687–703.

[34] Klaus-Jürgen Bathe. "Finite element method". In: *Wiley encyclopedia of computer science and engineering* (2007), pp. 1–12.

[35] George Turin. "An introduction to matched filters". In: *IRE transactions on Information theory* 6.3 (1960), pp. 311–329.

[36] Boualem Boashash and Ghasem Azemi. "A review of time–frequency matched filter design with application to seizure detection in multichannel newborn EEG". In: *Digital Signal Processing* 28 (2014), pp. 28–38.

[37] Itaf Ben Slimen, Larbi Boubchir, and Hassene Seddik. "Epileptic seizure prediction based on EEG spikes detection of ictal-preictal states". In: *Journal of biomedical research* 34.3 (2020), p. 162.